

Effects of Mounting on Accelerometer Response

Technical Paper 218
By George Stathopoulos

By **GEORGE STATHOPOULOS**

Chief, Environmental Simulation Div.
U. S. Naval Ordnance Lab.
White Oak
Silver Spring, Md.



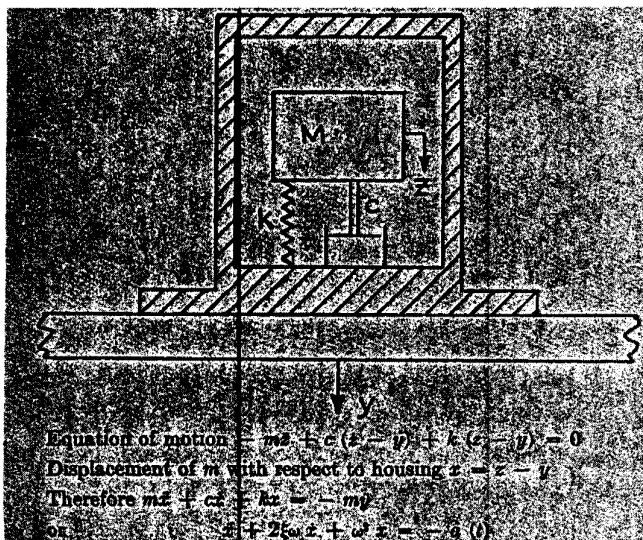
In the many words that have been written about accelerometers the mounting aspect has been mentioned only lightly. If the mounting is not given careful consideration, however, the response may be severely distorted. In extreme cases, the readings may even be worthless.

Effects of Mounting on Accelerometer Response

ACCCELEROMETERS have received widespread editorial coverage. However, one aspect in their application has been explored only lightly. It is the effect of the mount on which the accelerometer is fastened. Under some conditions the mount responds so that the accelerometer response faithfully reproduces the input acceleration. Under other conditions the mount distorts the accelerometer response, making the recording worthless.

Except for a few instances, in which the shock motion of a body can be studied by direct comparison of its position with respect to a stationary reference, most of the shock measurements are made with ac-

Fig. 1: Almost all accelerometers are like the one shown here. The basic equations associated with this unit are listed below.



celerometers mounted on the body under study. The accelerometer may be an electromechanical type which converts its response into an electrical signal. Or, it may be a strictly mechanical type which scribes its intelligence on a rotating surface or on a stationary surface, in which case only the peak response is obtained. In either case, almost all the pickups are single-degree-of-freedom systems (Fig. 1). Their performance can be determined from the differential equation:

$$\ddot{x} + 2\xi\omega\dot{x} + \omega^2x = -a(t) \quad (1)$$

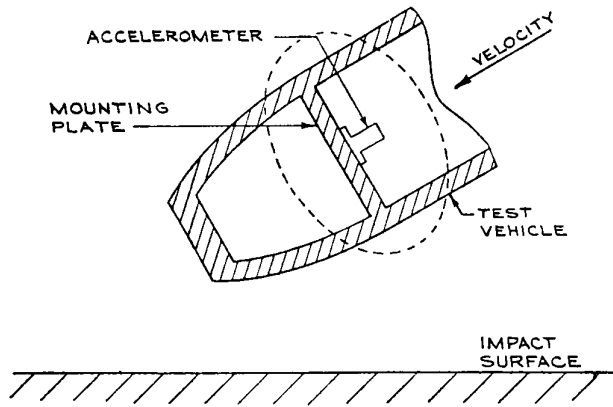
Many types of pickups such as the piezoelectric, bonded strain gages, and the mechanical gages do not employ damping. Others such as the unbonded strain gage, do, but find it difficult to provide effective damping in the high shock range. In these instances Eq. 1 reduces to:

$$\ddot{x} + \omega^2x = -a(t) \quad (2)$$

The remarks in the remainder of this article are devoted to the pickups whose motion is described by Eq. 2.

Basic Equation and Solution

Eqs. 1 and 2 have been studied by many authors. Refs. 1 and 2 are two of the more complete works in this field. In applying the results of these works, it is tacitly assumed that the structure on which the accelerometer was mounted faithfully transmitted the shock input to the accelerometer. This assumption is not valid for all loading situations. This can be seen by considering the case when the natural period of the plate is longer than the rise time of the input pulse. Here, the plate does not have a frequency response high enough to follow the input pulse and, hence, dis-



Accelerometer Mountings

torts it. Since the accelerometer is mounted to the plate, it can only respond to the motion of the plate. Therefore, it cannot give an accurate indication of the input shock. However, knowing the characteristics of the accelerometer mount, as well as the accelerometer, we can determine, with some degree of accuracy, the actual input to the structure under study.

A typical application is given in Fig. 2. For many situations the equivalent mechanical system is given by Fig. 3. The resulting equations of motion are:

$$\begin{cases} m_m \ddot{x}_m + (k_m + k_a) x_m - k_a x_a = k_m y \\ -k_a x_m + m_a \ddot{x}_a + k_a x_a = 0 \end{cases} \quad (3)$$

The response of the accelerometer is the displacement of its mass, x_a , relative to its housing. In the case under study, the housing is firmly attached to the plate. Therefore, the accelerometer response, x , is given by:

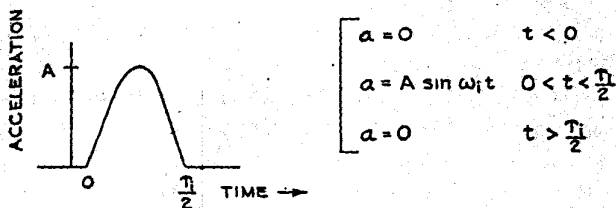
$$x = x_a - x_m$$

The acceleration indicated by the accelerometer in Laplace form is:

$$\bar{a}_a = -\omega_a^2 \bar{x} = \frac{\omega_a^2 \omega_m^2 \bar{a}}{p^4 + \left[\omega_m^2 + \omega_a^2 \left(1 + \frac{m_a}{m_m} \right) \right] p^2 + \omega_a^2 \omega_m^2} \quad (4)$$

In all practical cases with which we are concerned

Fig. 4: A half-sine pulse input with the associated math.



Laplace transform of input pulse.

$$\begin{aligned} \bar{a} &= \int_0^{\infty} a(t) e^{-pt} dt = \int_0^{\frac{T}{2}} A \sin \omega_1 t e^{-pt} dt \\ \bar{a} &= \frac{A}{p^2 + \omega_1^2} \left[1 + e^{-p \frac{T}{2}} \right] \end{aligned}$$

Fig. 2 (r.): Sketch illustrates a typical accelerometer application.

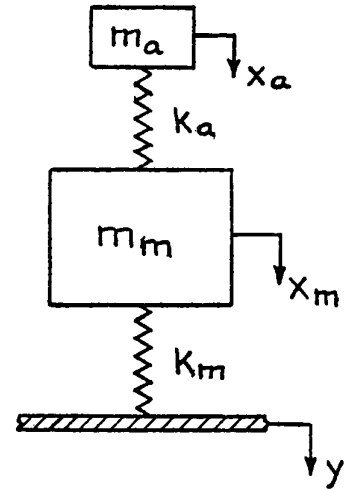


Fig. 3 (r.): The equivalent mechanical system of the encircled portion of Fig. 2.

in acceleration measurements, the ratio m_a/m_m is very small. (Some of the newer piezoelectric pickups weigh only a few grams.) For the case under study, assume that this ratio is 0.01.

In order to study Eq. 4, it is necessary to assume an input acceleration. A pulse that has proven quite useful is the half-sine pulse shown in Fig. 4. The time solution to Eq. 4 is:

$$a_a = \frac{A \omega_m^2 \omega_a^2 \omega_i}{(\omega_i^2 - \omega_m^2)(\omega_a^2 - \omega_m^2)(\omega_i^2 - \omega_a^2)} \left[\frac{\omega_i^2 - \omega_a^2}{\omega_m} \sin \omega_m t + \frac{\omega_a^2 - \omega_m^2}{\omega_i} \sin \omega_i t - \frac{\omega_i^2 - \omega_m^2}{\omega_a} \sin \omega_a t \right] \quad (5)$$

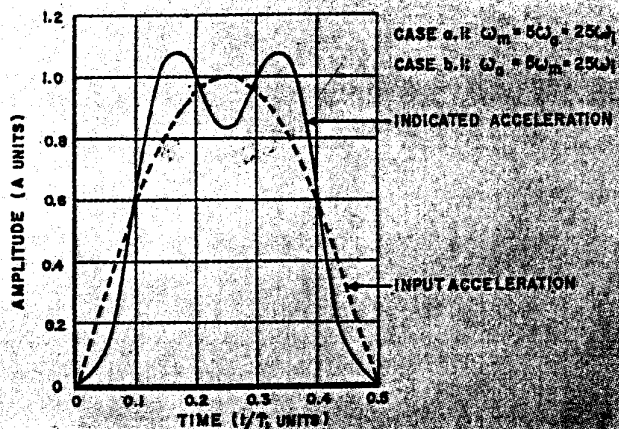
for $t > \frac{\tau_i}{2}$

$$a_a = \frac{A \omega_m^2 \omega_a^2 \omega_i}{(\omega_i^2 - \omega_m^2)(\omega_a^2 - \omega_m^2)(\omega_i^2 - \omega_a^2)} \left[\frac{\omega_i^2 - \omega_a^2}{\omega_m} \left\{ \sin \omega_m t + \sin \omega_m \left(t - \frac{\tau_i}{2} \right) \right\} - \frac{\omega_i^2 - \omega_m^2}{\omega_a} \left\{ \sin \omega_a t + \sin \omega_a \left(t - \frac{\tau_i}{2} \right) \right\} \right] \quad (6)$$

Interpretation of Results

At first glance Eq. 5 and 6 appear hopelessly complex. However, by taking limiting cases some insight into the behavior of the system can be obtained. Table 1 presents this study.

Fig. 5: Input acceleration is reproduced for cases a. 1 & b. 1.



In establishing the relationships of Table 1 it was necessary to assume that one of the 3 frequencies involved was considerably higher than the other two and, in turn, a second frequency was considerably higher than the third, i.e.,

$$\omega_1 \gg \omega_2 \gg \omega_3, \text{ or } \tau_1 = k_1 \omega_2 = k_2 \omega_3$$

where k_1 and k_2 are large positive numbers and $k_2 \gg k_1$. Several calculations were made using Eq. 5 and 6 with the arbitrarily chosen parameters of $k_1 = 5$ and $k_2 = 25$. The values were chosen smaller than the above assumptions to determine the variations produced. The results are shown in Table 2. Plots of the above cases are presented in Figs. 5 through 7. The situations considered are related to realistic conditions in Table 3.

From Table 2 we see that for the a.2 and b.2 cases, the frequency restrictions are not as severe as indicated by the analysis. For the frequency conditions chosen, the indicated velocity changes were within 1% of the actual. For cases a.1 and b.1, the indicated

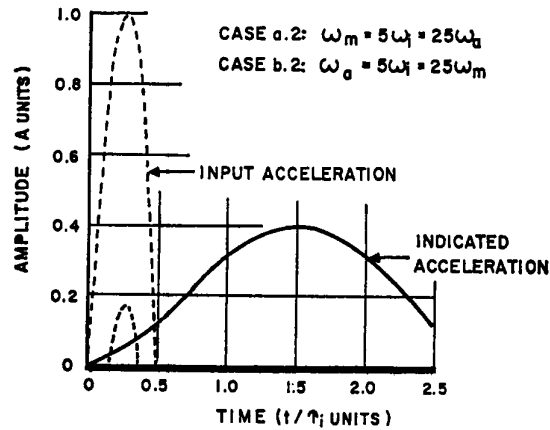


Fig. 6: Indicated acceleration is not the same as input for cases a. 2 & b. 2.

peak acceleration was 8% greater than the actual, and the resulting pulse shape was considerably distorted (Fig. 5). For cases c.1 and c.2, the indicated velocity change was 6% greater than that indicated by the analysis.

Concluding Remarks

From the preceding analysis, we see that the effect of the mount is very important. It must be considered in planning and analyzing shock measurements. As a minimum effort, the important frequencies of the mounting surfaces should be determined from either shock or vibration inputs. Before complete quantitative analyses on the effects of the mounting can be made, a large number of numerical solutions to Eq. 5 and 6 are required. The effects of different pulse shapes also should be determined.

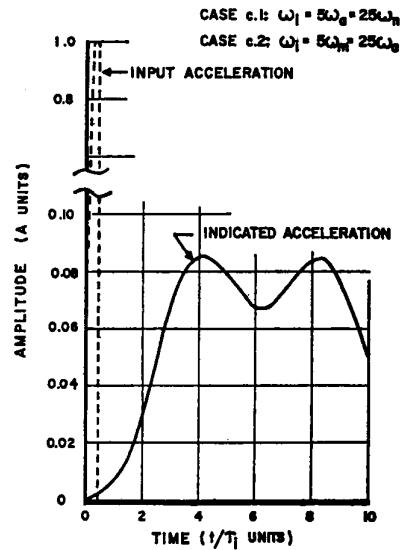


Fig. 7: Cases c.1 & c. 2 do not follow the input acceleration.

Table 1

Case	Freq. Relationship	Output	Remarks
a.1	$\omega_m \gg \omega_a \gg \omega_i$	$a_a = A \sin \omega_i t \quad 0 < t < \frac{\tau_i}{2}$ $a_a = 0 \quad t > \frac{\tau_i}{2}$	Input reproduced exactly.
a.2	$\omega_m \gg \omega_i \gg \omega_a$	a_a is very small $0 < t < \frac{\tau_i}{2}$ $(a_a)_{max.} = \omega_a \Delta V \quad t > \frac{\tau_i}{2}$	Max. indicated acceleration divided by accelerometer natural frequency equals velocity change of input pulse.
b.1	$\omega_a \gg \omega_m \gg \omega_i$	$a_a = A \sin \omega_i t \quad 0 < t < \frac{\tau_i}{2}$ $a_a = 0 \quad t > \frac{\tau_i}{2}$	Input reproduced exactly.
b.2	$\omega_a \gg \omega_i \gg \omega_m$	a_a is very small $0 < t < \frac{\tau_i}{2}$ $(a_a)_{max.} = \omega_m \Delta V \quad t > \frac{\tau_i}{2}$	Max. indicated acceleration divided by plate circular natural frequency equals velocity change of input pulse.
c.1	$\omega_i \gg \omega_a \gg \omega_m$	a_a is very small $0 < t < \frac{\tau_i}{2}$ $(a_a)_{max.} = \omega_m \Delta V \quad t > \frac{\tau_i}{2}$	Same as b.2.
c.2	$\omega_i \gg \omega_m \gg \omega_a$	a_a is very small $0 < t < \frac{\tau_i}{2}$ $(a_a)_{max.} = \omega_a \Delta V$	Same as a.2.

simple systems to the shock motion (Fig. 30). Examination of Figures 28 and 29 shows that the

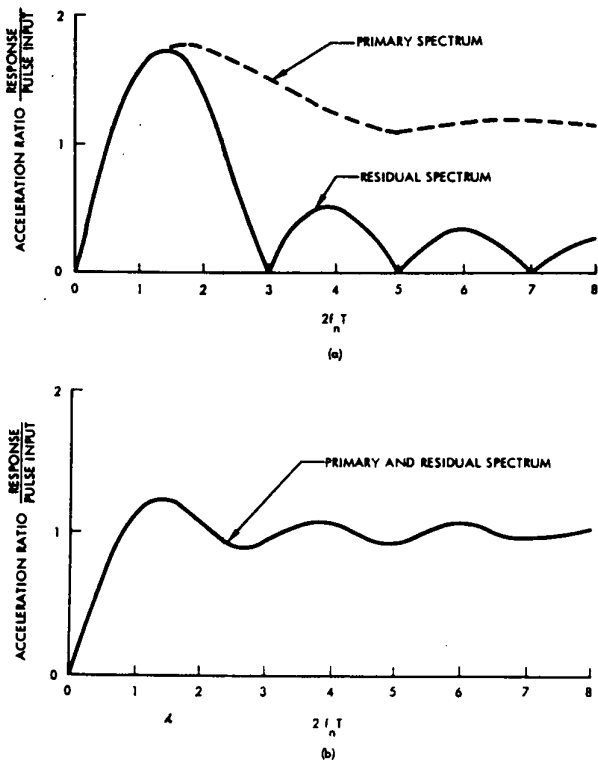
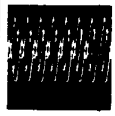


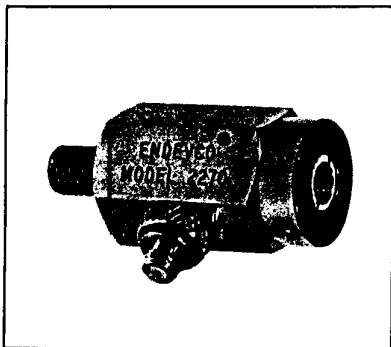
Figure 30. Shock spectrum of: (a) a half sine pulse of period T, and (b) a terminal peak sawtooth of period T (after Lowe).

response of a system during application of a shock may differ considerably from the residual motion after the shock input has ended. Because of this, it is customary to consider the primary spectrum (response during shock input) and the residual spectrum (response after shock input) separately. The primary spectrum defines a response that always has the same direction as the applied acceleration, while the residual spectrum defines peak acceleration in both directions. The residual spectrum is important not only in providing more information about dynamic loading, but because it also indicates the fatigue loading due to flexural motion. In view of this, it can be seen that a shock test that provides a flat response in both the primary and residual spectra would be highly desirable. Such a test would be equally severe in the loading it imposes on all equipments tested, regardless of their natural frequencies. Further, a spectrum that rises smoothly to about 100 Hz and is flat for all higher frequencies is a very good average of the shocks actually encountered in transporting and handling equipment. A terminal peak sawtooth acceleration pulse exhibits a spectrum of this type. In addition, the primary and residual spectra are almost equal (Fig. 30b).

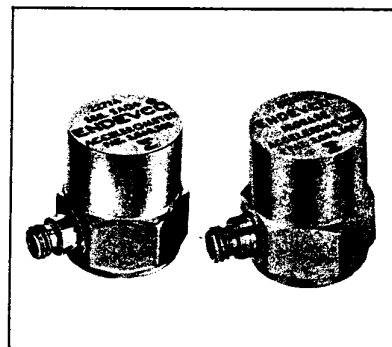
Shock spectra can be used to compare intensities of different shocks and are directly applicable to several dynamic design techniques, and the numbers quoted correlate better with the damage potential of the related shock. The difficult job of placing tolerances on pulse shapes is avoided and tests can be conducted that compare very well with actual field conditions. One of its great values is that it permits useful analysis of complex shock. It should be remembered that the shock spectrum tells what a shock does, not what it is.

ENDEVCO PRODUCTS RELATED TO THIS ARTICLE



Model 2270
Primary Standard Accelerometer
 The Model 2270 Accelerometer Standard is a combination accelerometer and calibration fixture for performing comparison calibration on other accelerometers. Extremely high stability is achieved by use of Piezite® Type P-10 crystal element. When calibrated by the reciprocity method, an absolute calibration, the error in sensitivity of the Model 2270 is $\pm 0.5\%$ at 100 Hz. Adapters provide for mounting test accelerometers with a variety of stud sizes. Calibration ranges are 5 Hz to 10,000 Hz and 0.2 g to 10,000 g.



Model 2271A and 2275
Precision Isobase®
Accelerometers
 The Models 2271A and 2275 piezoelectric accelerometers feature extremely low output sensitivity to strain or the bending of their mounting surface. Their wide and useful dynamic characteristics of 2 Hz to 5500 Hz and 0 to 10,000 g permit them to be used for most shock and vibration measurements. Transverse sensitivity is very low, 2% maximum. Flat charge-temperature response, $\pm 3\%$ nominal, over the range of -300°F. to $+500^\circ\text{F.}$, is achieved with Piezite® Type P-10 crystal material.



10869 NC Highway 903, Halifax, NC 27839 USA

endevco.com | sales@endevco.com | 866 363 3826

© 2022 PCB Piezotronics - all rights reserved. PCB Piezotronics is a wholly-owned subsidiary of Amphenol Corporation. Endevco is an assumed name of PCB Piezotronics of North Carolina, Inc., which is a wholly-owned subsidiary of PCB Piezotronics, Inc. Accumetrics, Inc. and The Modal Shop, Inc. are wholly-owned subsidiaries of PCB Piezotronics, Inc. IMI Sensors and Larson Davis are Divisions of PCB Piezotronics, Inc. Except for any third party marks for which attribution is provided herein, the company names and product names used in this document may be the registered trademarks or unregistered trademarks of PCB Piezotronics, Inc., PCB Piezotronics of North Carolina, Inc. (d/b/a Endevco), The Modal Shop, Inc. or Accumetrics, Inc. Detailed trademark ownership information is available at www.pcb.com/trademarkownership.

TP218-011922